Sue *et al. Journal of Ovarian Research* (2024) 17:187
https://doi.org/10.1186/s13048-024-01509-x

Journal of Ovarian Research

RESEARCH Open Access

The synergistic mechanisms of propofol with cisplatin or doxorubicin in human ovarian cancer cells

Sung-How Sue[1], Wei-Cheng Tseng[2], Zih-Syuan Wu[3], Shih-Ming Huang[3,4], Jia-Lin Chen[2*], Zhi-Fu Wu[5,6,7*] and Hou-Chuan Lai[2*]

Abstract

Background Most ovarian cancer cases are diagnosed at an advanced stage, leading to poor outcomes and a relatively low 5-year survival rate. While tumor resection in the early stages can be highly effective, recurrence following primary treatment remains a significant cause of mortality. Propofol is a commonly used intravenous anesthetic agent in cancer resection surgery. Previous research has shown that propofol anesthesia was associated with improved survival in patients undergoing elective surgery for epithelial ovarian cancer. However, the underlying antitumor mechanisms are not yet fully understood.

Methods This study aimed to uncover the antitumor properties of propofol alone and combined with cisplatin or doxorubicin, in human SKOV3 and OVCAR3 ovarian cancer cells. We applied flowcytometry analysis for mitochondrial membrane potential, apoptosis, and autophagy, colony formation, migration, and western blotting analysis.

Results Given that chemotherapy is a primary clinical approach for managing advanced and recurrent ovarian cancer, it is essential to address the limitations of current chemotherapy, particularly in the use of cisplatin and doxorubicin, which are often constrained by their side effects and the development of resistance. First of all, propofol acted synergistically with cisplatin and doxorubicin in SKOV3 cells. Moreover, our data further showed that propofol suppressed colony formation, disrupted mitochondrial membrane potential, and induced apoptosis and autophagy in SKOV3 and OVCAR3 cells. Finally, the effects of combined propofol with cisplatin or doxorubicin on mitochondrial membrane potential, apoptosis, autophagy, and epithelial-mesenchymal transition were different in SKOV3 and OVCAR3 cells, depending on the p53 status.

Conclusion In summary, repurposing propofol could provide novel insights into the existing chemotherapy strategies for ovarian cancer. It holds promise for overcoming resistance to cisplatin or doxorubicin and may

*Correspondence:
Jia-Lin Chen
babe.ane@gmail.com
Zhi-Fu Wu
aneswu@gmail.com
Hou-Chuan Lai
m99ane@gmail.com

Full list of author information is available at the end of the article

© The Author(s) 2024. **Open Access** This article is licensed under a Creative Commons Attribution-NonCommercial-NoDerivatives 4.0 International License, which permits any non-commercial use, sharing, distribution and reproduction in any medium or format, as long as you give appropriate credit to the original author(s) and the source, provide a link to the Creative Commons licence, and indicate if you modified the licensed material. You do not have permission under this licence to share adapted material derived from this article or parts of it. The images or other third party material in this article are included in the article's Creative Commons licence, unless indicated otherwise in a credit line to the material. If material is not included in the article's Creative Commons licence and your intended use is not permitted by statutory regulation or exceeds the permitted use, you will need to obtain permission directly from the copyright holder. To view a copy of this licence, visit http://creativecommons.org/licenses/by-nc-nd/4.0/.

potentially reduce the required chemotherapy dosages and associated side effects, thus improving treatment outcomes.

Keywords Ovarian cancer, Propofol, Cisplatin, Doxorubicin, Combinatory therapy

Introduction

Ovarian cancer is a significant global health concern, ranking as the seventh most common cancer and the eighth leading cause of cancer-related mortality among women worldwide [1, 2]. Primary ovarian tumors are classified into four primary groups, based on their distinct biological and molecular characteristics: epithelial, mesenchymal, sex cord-stromal, or germ cell in origin. The most prevalent among them is epithelial ovarian cancer, which accounts for approximately 90% of all ovarian malignancies [3]. Most ovarian cancer cases are diagnosed at an advanced stage, which leads to poor outcomes of the disease, complicated with a 5-year survival rate of only 46% after diagnosis [4]. The primary treatment approach for ovarian cancer patients typically involves surgical tumor removal, often complemented by a combination of radiotherapy and chemotherapy. Despite the effectiveness of early stages tumor resection, ovarian cancer recurrence post-surgery remains a significant mortality factor. Tumor cells have the potential to disseminate to distant organs and trigger regrowth and recurrence via vascular and lymphatic system infiltration during surgery [5, 6]. Surgical procedures can inadvertently spread cancer cells, leading to a higher risk of recurrence [7]. Additionally, they can suppress the immune system and the host's tumor response, creating a favorable microenvironment for residual and circulating cancer cells to proliferate after the operation [8]. The choice of anesthetic drugs or techniques during cancer surgery might impact the tumor microenvironment and cancer progression by influencing perioperative inflammatory or immune responses [9–12]. This, in turn, could affect the prognosis of cancer patients, suggesting that specific anesthetic selection may play a role in cancer recurrence [5, 6]. Consequently, there is a growing focus on understanding how anesthetic drugs influence the outcomes of ovarian cancer patients.

Propofol, a commonly used intravenous anesthetic that mainly works via the γ-aminobutyric acid A receptor in the central nervous system, is widely administered in various clinical surgical settings, including cancer surgery, with the advantages of rapid onset, a short duration of action, rapid elimination, and low incidences of postoperative nausea and vomiting [13]. In addition to several anesthetic benefits, propofol also demonstrates antitumor effects by not only suppressing the malignancy of human cancers, but also altering the resistance to chemotherapeutic agents [13–15]. In our previous study, we found a correlation between propofol anesthesia and improved survival outcomes among patients undergoing elective open surgery for epithelial ovarian cancer [16]. Hence, it is crucial to explore the potential of repurposing the antitumor activity of propofol, elucidating its detailed mechanisms of action both independently or in combination with current chemotherapy.

Chemotherapy is the first choice for clinical treatment to manage advanced and recurrent ovarian cancers. Cisplatin, an alkylating agent, is widely utilized as a chemotherapeutic agent for treating ovarian cancer, as well as for testicular, bladder, and lung cancers [17]. It induces DNA damage by forming cisplatin-DNA adducts, leading to cell cycle arrest and apoptosis [18, 19]. However, platinum-refractory ovarian cancer remains incurable [20]. Elucidating cisplatin resistance in ovarian cancers is challenging due to the diverse resistance mechanisms that have been identified in a variety of cancers (in PubMed, more than 18640 papers match the search term "cisplatin resistance"). Cancer cells often develop resistance to cisplatin through three main molecular mechanisms: increased DNA repair, altered cellular accumulation, and increased drug inactivation [21]. Therefore, predicting and treating cisplatin resistance is challenging due to its complex mechanisms. Doxorubicin, an anthracycline analogue, is one of the modalities used as a single-agent treatment for relapsed ovarian cancers [22]. It functions by halting the process of replication via the stabilization of the DNA–topoisomerase II complex, preventing the resealing of the DNA double helix after it has been broken for replication [23]. It is a highly active anticancer agent in many different clinical settings, and its primary side effect is cardiotoxicity. The limitations of using cisplatin and doxorubicin lie in their side effects and the development of resistance. The use of combination anticancer therapies is compelling in clinical practice for several reasons [24, 25]. Firstly, combined drug regimens can reduce overall toxicity by allowing the use of individual drugs at lower dosages while maintaining therapeutic efficacy. Secondly, combination therapies can help reduce the emergence of drug resistance by concurrently targeting multiple molecular pathways essential for cancer cell survival and disrupting cellular mechanisms associated with adaptive resistance. Thirdly, combining therapies can enhance treatment outcomes, leading to superior therapeutic effects, particularly when a synergistic anticancer activity is achieved. Additionally, this approach can overcome clonal heterogeneity, which is linked to improved response rates. Therefore, combination chemotherapy is an effective strategy, and the addition of a

chemo-sensitizer and side-effect mitigator could potentially benefit ovarian cancer patients.

Optimal first-line clinical applications for advanced ovarian cancer include histopathological diagnosis, accurate surgical staging, debulking surgery, and platinum-based chemotherapy. The role of anesthetics as a chemo-sensitizer provides a new combination therapy for current first-line management approaches for advanced ovarian cancer. This study aimed to determine the antitumor properties of propofol, including its impact on cell growth, viability, and migration, as well as to assess the synergistic effects of propofol when combined with cisplatin or doxorubicin in enhancing chemosensitivity in human ovarian cancer cell lines. In addition to maintaining the integrity of immunity and reducing the tendency toward cancer metastasis [26, 27], repurposing of propofol could offer novel insights into current chemotherapy approaches for ovarian cancer, with the potential to overcome resistance to cisplatin or doxorubicin, or to reduce chemotherapy dosages and associated side effects.

Materials and methods

Cell culture and reagents

SKOV3 (ATCC®HTB-77™) and OVCAR3 cells (ATCC®HTB-161™) were sourced from the American Type Culture Collection (ATCC; Manassas, VA, USA). We cultured these cells in Roswell Park Memorial Institute (RPMI) 1640 medium supplemented with 10% fetal bovine serum (FBS) and 1% penicillin–streptomycin (Thermo Fisher Scientific, Waltham, MA, USA). These two cell lines were regularly monitored to ensure mycoplasma-free cells, and regularly monitored with short-tandem-repeat profiling for their identities. The chemicals used, including propofol, doxorubicin, cisplatin, propidium iodide (PI), acridine orange (AO), and thiazolyl blue tetrazolium bromide (MTT), were obtained from Sigma Aldrich (Sigma Aldrich; St. Louis, MO, USA).

Cell survival analysis

The cells were seeded into 96-well plates and exposed to combinations of propofol with either cisplatin or doxorubicin for a 24-hour period. SKOV3 cells were treated with 0, 0.625, 1.25, 2.5, 5, 10, 20, 40, 80, and 160 μg/ml propofol combined with 0, 1.5625, 3.125, 6.25, 12.5, 25, 50, and 100 μM cisplatin or 0, 0.625, 1.25, 2.5, 5, 10, 20, and 40 μM doxorubicin for 24 h. OVCAR3 cells were treated with 0, 0.390625, 0.78125, 1.5625, 3.125, 6.25, 12.5, 25, 50, and 100 μg/ml propofol combined with 0, 1.25, 2.5, 5, 10, 20, 40, and 80 μM cisplatin or 0, 0.078125, 0.15625, 0.3125, 0.625, 1.25, 2.5, and 5 μM doxorubicin for 24 h. Subsequently, 0.5 mg/ml MTT solution was added to each well, and the cells were incubated for at least 1 h. After removing the MTT solution, 100 μl of dimethyl sulfoxide (DMSO) was added to each well. The absorbances at 570 nm and 650 nm were measured using an ELISA plate reader (Multiskan EX, Thermo Fisher Scientific, Waltham, MA, USA). The combination index (CI) was calculated using CalcuSyn (Biosoft, Cambridge, UK) to generate an isobologram. CI values of 1, <1, and >1 indicate additive, synergistic, and antagonistic effects, respectively.

Colony formation assay

The cells were plated into 6-well cell culture plates at a density of 2000 cells per well and allowed to incubate overnight. Subsequently, the cells were treated with 10, 30, and 50 μg/ml propofol and incubated for a period of 14 days. Following the incubation, the cells were stained with a 0.005% crystal violet solution for 1 h. After air drying, the colonies were photographed and counted.

Apoptosis assay

Apoptosis was analyzed utilizing the PE Annexin-V apoptosis detection kit (BD Pharmingen, San Diego, California, USA) with 7-AAD, following the manufacturer's protocol. The FACSCalibur flow cytometer and Cell Quest Pro software (BD Biosciences, Franklin Lakes, NJ, USA) were employed to measure and quantify the apoptotic ratio.

Mitochondrial membrane potential assay

Following treatment with 10, 30, and 50 μg/ml propofol in combination with 10 μM cisplatin or 1 μM doxorubicin, both dead and live cells were collected. Subsequently, JC-1 solution (BD Pharmingen) was added, and the cells were incubated for 15 min. Afterward, the cells were washed twice with a binding buffer. Each sample was analyzed using the FACSCalibur flow cytometer and Cell Quest Pro software.

Acridine Orange Staining for autophagy analysis

After treating the cells with a combination of 10, 30, and 50 μg/ml propofol with 10 μM cisplatin or 1 μM doxorubicin, AO was applied at a concentration of 1 μg/ml for 30 min. Then, the cells were washed with PBS. Subsequently, the stained cells were visualized and photographed using a fluorescence microscope. For imaging, a filter block containing a 465- to 495-nanometer bandpass excitation filter, a 505-nanometer dichroic mirror, and a 590-nanometer long-pass barrier filter was used. For flow cytometry analysis, the fluorescence intensities of 10,000 cells per sample were measured using the FACSCalibur flow cytometer and Cell Quest Pro software.

Cell cycle profiles

After treatment with 10, 30, and 50 μg/ml propofol in combination with 10 μM cisplatin or 1 μM doxorubicin, the treated cells were trypsinized and washed with PBS.

Then, the cell pellet was resuspended in 1 ml of PBS and fixed in 5 ml of 70% ice-cold ethanol, which was stored at -30 °C overnight. On the following day, the cells were washed twice with ice-cold PBS containing 1% FBS. Subsequently, they were stained with a PI staining solution (5 μg/ml PI in PBS, 0.5% Triton X-100, and 0.5 μg/ml RNase A) for 30 min. Each sample was analyzed using the FACSCalibur flow cytometer and Cell Quest Pro software.

Migration assay

The cells were seeded into 12-well plates at a density of 8×10^4 cells per well to achieve confluent monolayers. Straight wounds were created using 200-microliter pipette tips. After washing the plates with medium to eliminate cell debris, the wounded monolayers were treated with 30 and 50 μg/ml propofol. The wound gaps were photographed at regular intervals (0 and 24 h), and the cell-free wound areas were quantified using ImageJ software.

Western blot

The cells were lysed in a RIPA (radio-immunoprecipitation assay) cell lysis buffer for protein extraction. Equal amounts of protein were determined for SDS-PAGE analysis. Then, the proteins were transferred to PVDF membranes and blocked with 5% nonfat milk in TBST for 1 h. Following this, the membranes were incubated with primary antibodies overnight at 4 °C with shaking, and subsequently incubated with secondary antibodies for an additional 1 h at room temperature. The primary antibodies used in this study were obtained from the following sources: α-actinin (ACTN), α-tubulin, p53, and p62 from Santa Cruz Biotechnology (Santa Cruz, CA, USA); γ-H2A.x, cyclin D1, and α-SMA from Abcam (Cambridge, MA, USA); LC3B II, E-cadherin, p-ERK, ERK, Snail, and Vimentin from Cell Signaling (Danvers, MA, USA).

Statistical analysis

The results are presented as mean ± SD and are representative of three independent experiments. Student's *t*-tests were conducted for all group comparisons, with statistical significance set at $p<0.05$.

Results

Propofol acted synergistically with cisplatin and doxorubicin in SKOV3 human ovarian cancer cell lines and only acted synergistically with doxorubicin in OVCAR3 cells

By repurposing FDA-approved drug propofol, we could significantly shorten the time and reduce cost compared to de novo drug discovery [28]. Our primary goal was to examine the potential antitumor activities of propofol and determine whether it exhibits synergistic effects with cisplatin and doxorubicin in current clinical applications via a combination index analysis. Two human ovarian cancer cell lines, SKOV3 (p53-null) and OVCAR3 (p53 R248Q), were selected because of their relevance to p53-depedent cisplatin sensitivity [29, 30]. Hence, SKOV3 and OVCAR3 were applied for treatment with propofol alone or in combination with cisplatin or doxorubicin, followed by cell survival analysis (Fig. 1). Our data showed that the effective dose (ED50) values for SKOV3 cells were 54.6 μg/ml for propofol, 31.6 μM for cisplatin, and 0.8 μM for doxorubicin. For OVCAR3 cells, the ED50 values were 19 μg/ml for propofol, 9.4 μM for cisplatin, and 3.2 μM for doxorubicin. Propofol acted synergistically, with cisplatin or doxorubicin to suppress cell survival in SKOV3 cells (Fig. 1A and B), whereas propofol only acted synergistically with doxorubicin to suppress cell survival in OVCAR3 cells (Fig. 1C and D). In SKOV3 cells, propofol reduced the ED50 of cisplatin from 31.6 μM to 5.3 μM, and of doxorubicin from 0.8 μM to 0.38 μM (Fig. 1A and B). In OVCAR3 cells, propofol reduced the ED50 of doxorubicin from 3.2 μM to 0.1 μM (Fig. 1C and D).

Propofol suppressed cellular proliferation and induced apoptosis in SKOV3 and OVCAR3 human ovarian cancer cell lines

Since propofol exhibited antitumor activity and acted as a sensitizer for cisplatin- or doxorubicin-induced cytotoxicity in human ovarian cancer cells (Fig. 1). We further examined the role of propofol in cellular proliferation using colony formation analysis (Fig. 2). Our data showed that propofol significantly inhibited the cellular proliferation of SKOV3 and OVCAR3 cells in a dose-dependent manner (Fig. 2A and B for SKOV3 cells; 2 C and D for OVCAR3 cells). Next, our aim was to investigate whether the cytotoxicity induced by propofol resulted from an imbalance between cellular proliferation and apoptosis in human ovarian cancer cells. We further utilized annexin-V and 7-AAD to assess the status of early apoptosis, late apoptosis, and necrosis. Subsequently, we quantified the population of early and late apoptosis induced by propofol, cisplatin, or doxorubicin in SKOV3 and OVCAR3 cells (Fig. 3). In SKOV3 cells, propofol, cisplatin, or doxorubicin alone induced early apoptosis or/and late apoptosis (Fig. 3A and C). Propofol and doxorubicin significantly enhanced early apoptosis, late apoptosis, and total apoptosis, whereas the combination of propofol and cisplatin did not affect cellular apoptosis. In OVCAR3 cells, 50 μg/ml propofol induced both early and late apoptosis. Cisplatin suppressed propofol-induced early and late apoptosis, while doxorubicin enhanced the propofol-induced early apoptosis and suppressed the propofol-induced late apoptosis (Fig. 3B and C). Furthermore, cisplatin alone demonstrated no effect on early and late apoptosis, while

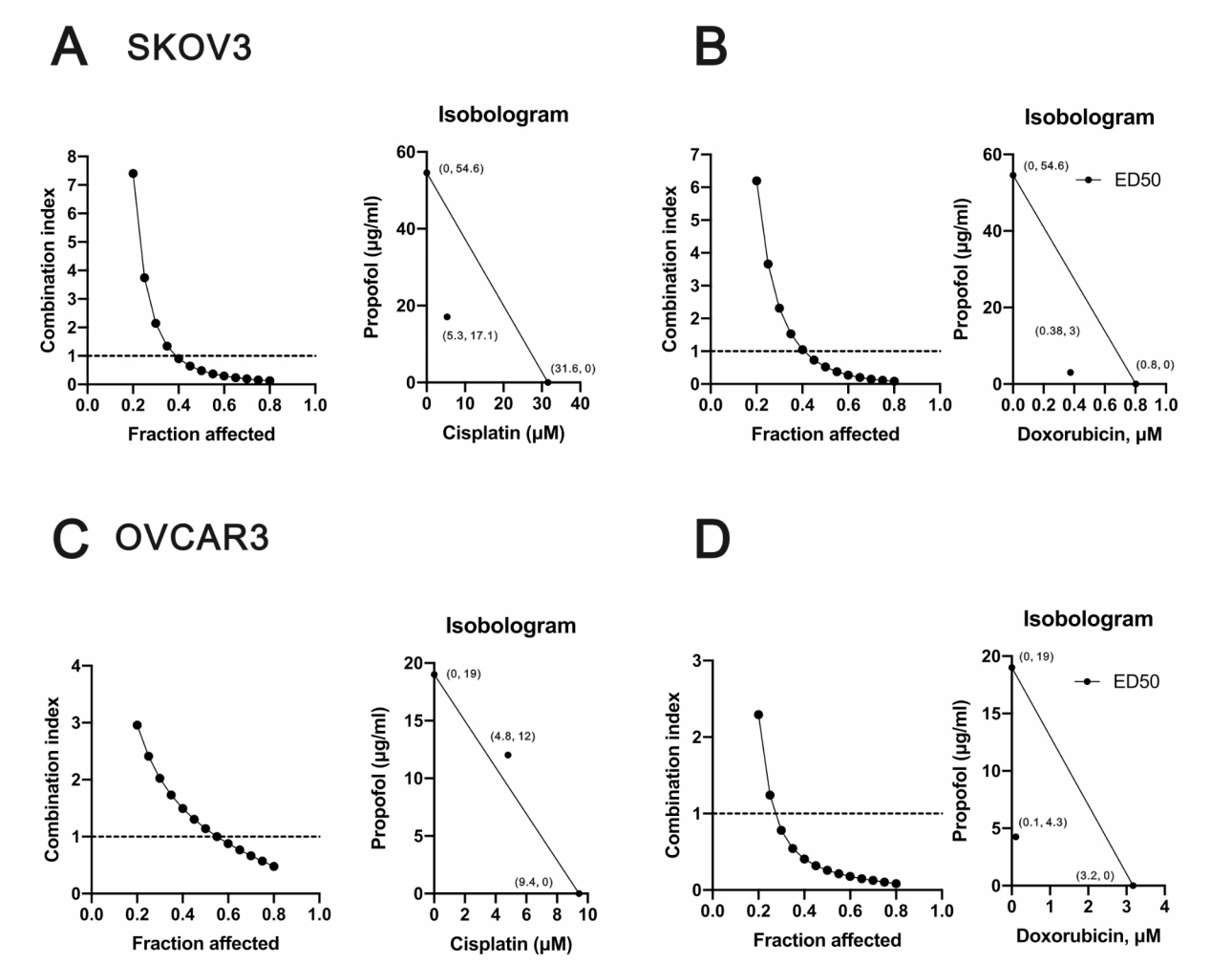

Fig. 1 The CI values were determined for the combination treatment of propofol with cisplatin or doxorubicin in human ovarian cancer cells. (**A and B**) SKOV3 cells were treated with 0, 0.625, 1.25, 2.5, 5, 10, 20, 40, 80, and 160 μg/ml propofol combined with (**A**) 0, 1.5625, 3.125, 6.25, 12.5, 25, 50, and 100 μM cisplatin or (**B**) 0, 0.625, 1.25, 2.5, 5, 10, 20, and 40 μM doxorubicin for 24 h. (**C and D**) OVCAR3 cells were treated with 0, 0.390625, 0.78125, 1.5625, 3.125, 6.25, 12.5, 25, 50, and 100 μg/ml propofol combined with (**C**) 0, 1.25, 2.5, 5, 10, 20, 40, and 80 μM cisplatin or (**D**) 0, 0.078125, 0.15625, 0.3125, 0.625, 1.25, 2.5, and 5 μM doxorubicin for 24 h. Cell viability was measured according to the MTT method. The experimental points below the line correspond to CI < 1, indicating a synergistic effect

doxorubicin alone suppressed early and late apoptosis in OVCAR3 cells. These findings suggested that 50 and 30 μg/ml propofol enhanced cisplatin-induced apoptosis in SKOV3 and OVCAR3 cells, respectively, while 50 μg/ml propofol enhanced doxorubicin-induced apoptosis in both human ovarian cancer cell lines.

Cisplatin and doxorubicin had different effects, in that propofol disrupted mitochondrial membrane potential and induced autophagy in SKOV3 and OVCAR3 cells

Mitochondrial dysfunction is one of the chemotherapy resistance characteristics of various cancer patients [31–34]. Numerous chemotherapeutic drugs, such as cisplatin and doxorubicin, target mitochondria as a part of their mechanism of action, contributing to the development of resistance [35]. Therefore, we aimed to investigate whether propofol enhanced the effects of cisplatin and doxorubicin in human ovarian cancer cells by inducing mitochondrial dysfunction. JC-1 dye was utilized to assess the intact status of mitochondrial membrane potential with red aggregates indicating intact mitochondrial membrane potential within the mitochondria, and green monomers indicating disruption of mitochondrial membrane potential. By monitoring the populations of red and green dyes, we analyzed the effects of propofol, cisplatin, and doxorubicin on mitochondrial membrane potential in SKOV3 and OVCAR3 cells (Fig. 4). In SKOV3 cells, only 50 μg/ml propofol disrupted mitochondrial membrane potential (Fig. 4A and B). We further observed that 10 μM cisplatin enhanced

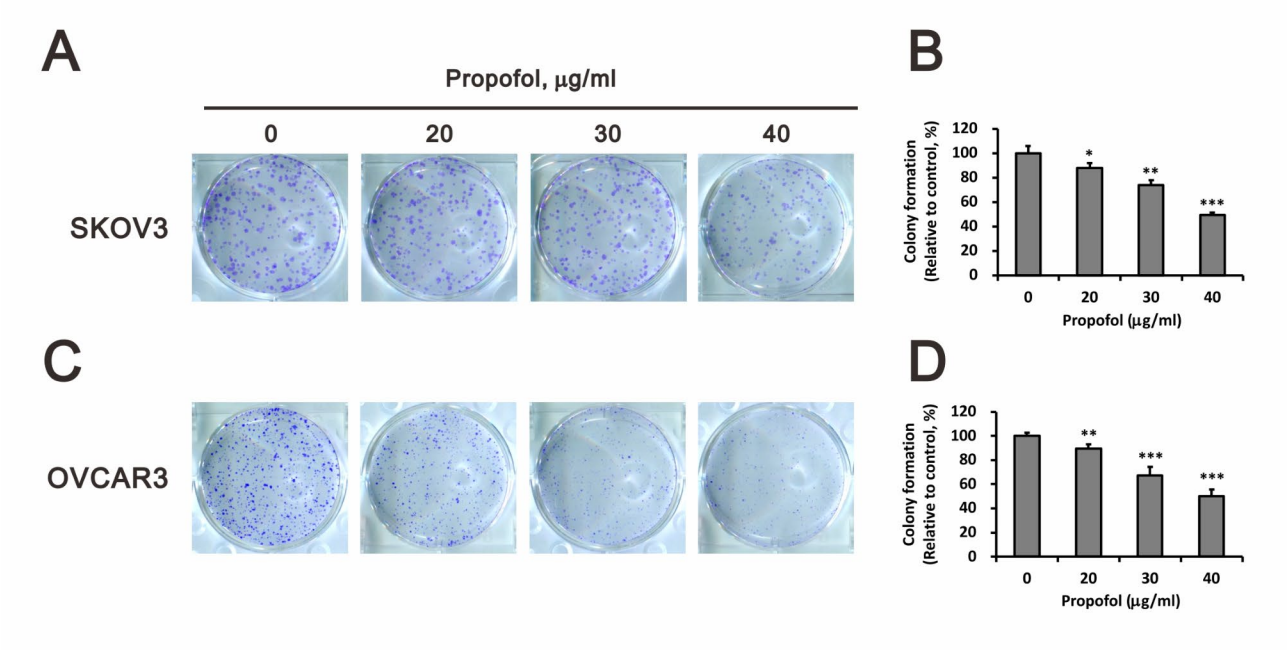

Fig. 2 Assessment of the impact of propofol on the colony-forming capability of human ovarian cancer cells. SKOV3 and OVCAR3 cells were exposed to varying concentrations of propofol (0, 20, 30, and 40 μg/ml) for a duration of 14 days. The bars represent the mean ± SD of three independent experiments. Statistical significance is indicated by * for $p < 0.05$, ** for $p < 0.01$, and *** for $p < 0.001$, determined using Student's *t*-tests

the disruption caused by 30 μg/ml and 50 μg/ml propofol, while doxorubicin further enhanced the disruption caused by 10 μg/ml propofol and suppressed the disruption caused by 50 μg/ml propofol. In OVCAR3 cells, only 50 μg/ml propofol disrupted mitochondrial membrane potential (Fig. 4C and D). Additionally, we further observed that 10 μM cisplatin enhanced the disruption caused by and suppressed the disruption caused by 50 μg/ml propofol. Doxorubicin had the ability to suppress the disruption caused by 50 μg/ml propofol.

Autophagy is characterized by sequestration of cellular organelles, such as mitophagy for mitochondria, and target proteins into autophagic vesicles which fuse with lysosomes [36, 37]. Basal autophagy plays an important role in the disposal of damaged subcellular organelles and protein aggregates, under normal conditions. Under starvation and reactive oxygen species stress conditions, autophagy supplies the cell with an internal source of nutrients for cells to adapt and survive in the face of unfavorable conditions [38, 39]. Acridine orange (AO) is a lysosomotropic green fluorescent dye that accumulates in acidic organelles. Upon protonation and trapped within the acidic organelles, it forms aggregates that emit bright red fluorescence. Hence, AO was applied to examine the status of autophagy in our study. We collected AO-stained images and subsequently quantified the red positive cells via fluorescent microscopy and flow cytometry analysis (Fig. 5). Our data showed that AO red positive cells were increased with propofol, cisplatin, and doxorubicin in SKOV3 cells. Propofol had the ability to elevate the population of AO red positive cells induced by cisplatin and doxorubicin (Fig. 5A and C). In OVCAR3 cells, only propofol induced autophagy, and further induced autophagy with 10 μM cisplatin at 30 μg/ml and 50 μg/ml (Fig. 5B and D). We examined the levels of autophagy biomarkers LC3B II and p62, modulated by propofol, cisplatin, and doxorubicin, using Western blotting analysis in SKOV3 and OVCAR3 cells (Fig. 5E and F). Our data showed that LC3B II proteins were increased by propofol alone and by propofol in combination with doxorubicin in SKOV3 cells (Fig. 5E). In OVCAR3 cells, the protein levels of LC3B II were increased by propofol, cisplatin, and doxorubicin. Furthermore, the induction by propofol was enhanced by cisplatin or suppressed by doxorubicin (Fig. 5F). The expression patterns of p62 proteins suggested that it played a role in the initiation of autophagy rather than serving as cargo for autophagolysosomes in these two cell types.

Cisplatin and doxorubicin had different effects on the cell cycle profiles driven by propofol in SKOV3 and OVCAR3 cells

Based on our previous data, we further examined the effects of propofol, cisplatin, and doxorubicin on the cell cycle profile, including the subG1 (for apoptosis) and S (for cellular proliferation) phases, in SKOV3 and OVCAR3 cells (Fig. 6). In SKOV3 cells, propofol induced the populations of the subG1 and S phases while reduced

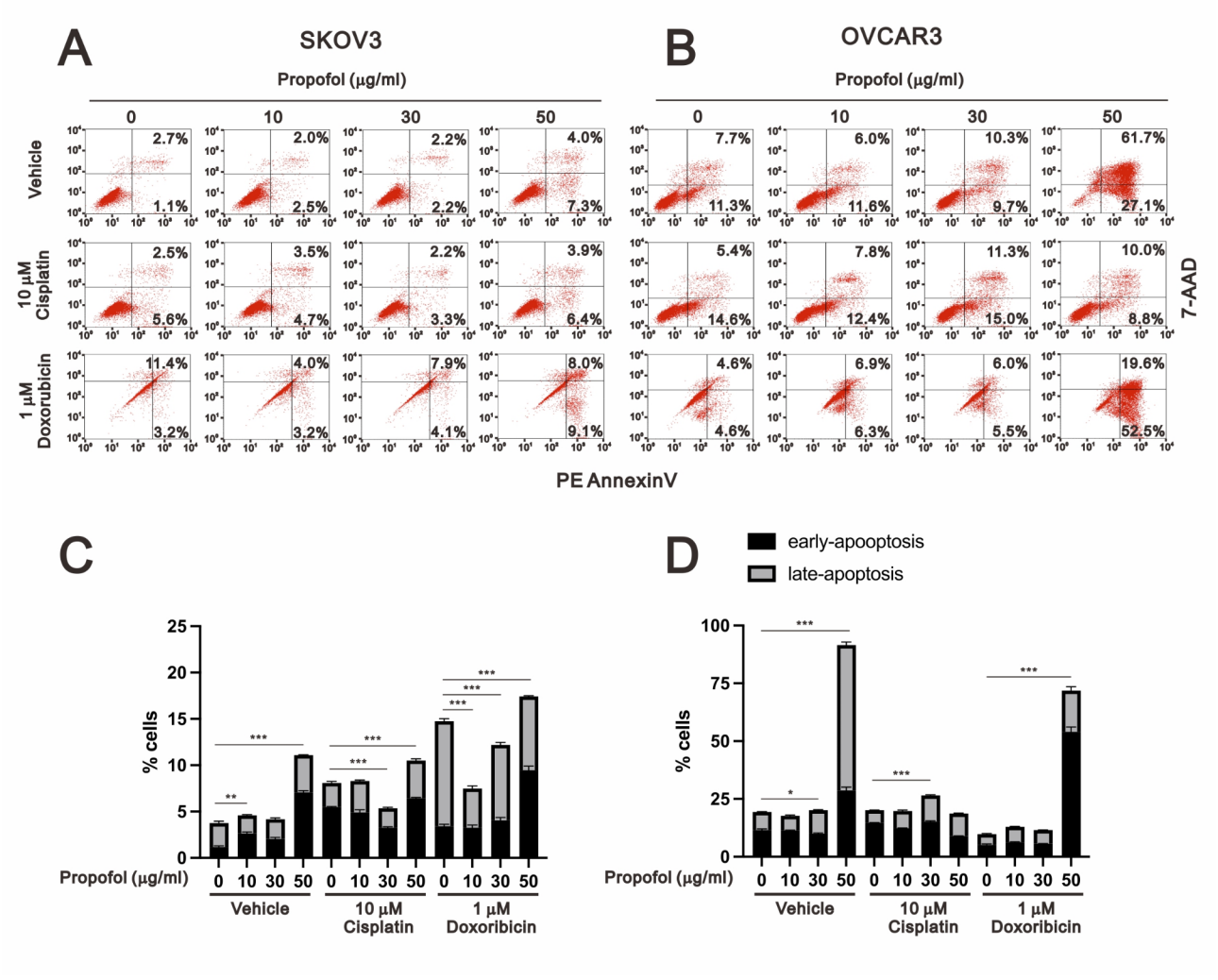

Fig. 3 Apoptotic effects were evaluated upon administering the combination treatment of propofol with cisplatin or doxorubicin in human ovarian cancer cells. SKOV3 and OVCAR3 cells were treated with different concentrations of propofol (0, 10, 30, and 50 μg/ml) in combination with either 10 μM cisplatin or 1 μM doxorubicin. The bars represent the mean ± SD of three independent experiments. Statistical significance is indicated by * for $p < 0.05$, ** for $p < 0.01$, and *** for $p < 0.001$, determined using Student's *t*-tests

the G2/M population (Fig. 6A). Cisplatin induced the populations of the subG1 and S phases and reduced the populations of the G1 and G2/M phases. Doxorubicin induced the populations of the subG1, S, and G2/M phases, and reduced the G1 population. The synergistic induction of subG1 populations were found in the combination of propofol with cisplatin and doxorubicin. Additionally, propofol had the ability to rescue the reductive effect of doxorubicin on the G1 phase. In OVCAR3 cells, propofol dramatically induced the population of the subG1 phase, accompanied with dramatic reductions in the G1, S, and G2/M populations (Fig. 6B). Cisplatin induced the population of the subG1 and reduced the populations of the G1 and G2/M phases. Doxorubicin had no effect on the subG1 phase, but dramatically induced the populations of the S and G2/M phases, accompanied by a reduction in the G1 population. Propofol co-treated with cisplatin or doxorubicin itself remained effective on the subG1 phase, accompanied by a reduction in these effects on G1, S, and G2/M by cisplatin or doxorubicin.

Propofol suppressed cellular migration and mediated different pathways in SKOV3 and OVCAR3 cells

Epithelial–mesenchymal transition (EMT) is one of the key elements to cancer cell dissemination, including cancer cell survival and metastasis, and chemoresistance, including cisplatin and doxorubicin [40]. E-cadherin is an epithelial cell marker, while vimentin is a mesenchymal cell marker [41]. The expression of E-cadherin is repressed by Snail, which is regulated by various signals, including the ERK pathway, TGF-β pathway, and p53. Hence, we examined the potential inhibitory effect of propofol on EMT using migration assay in human

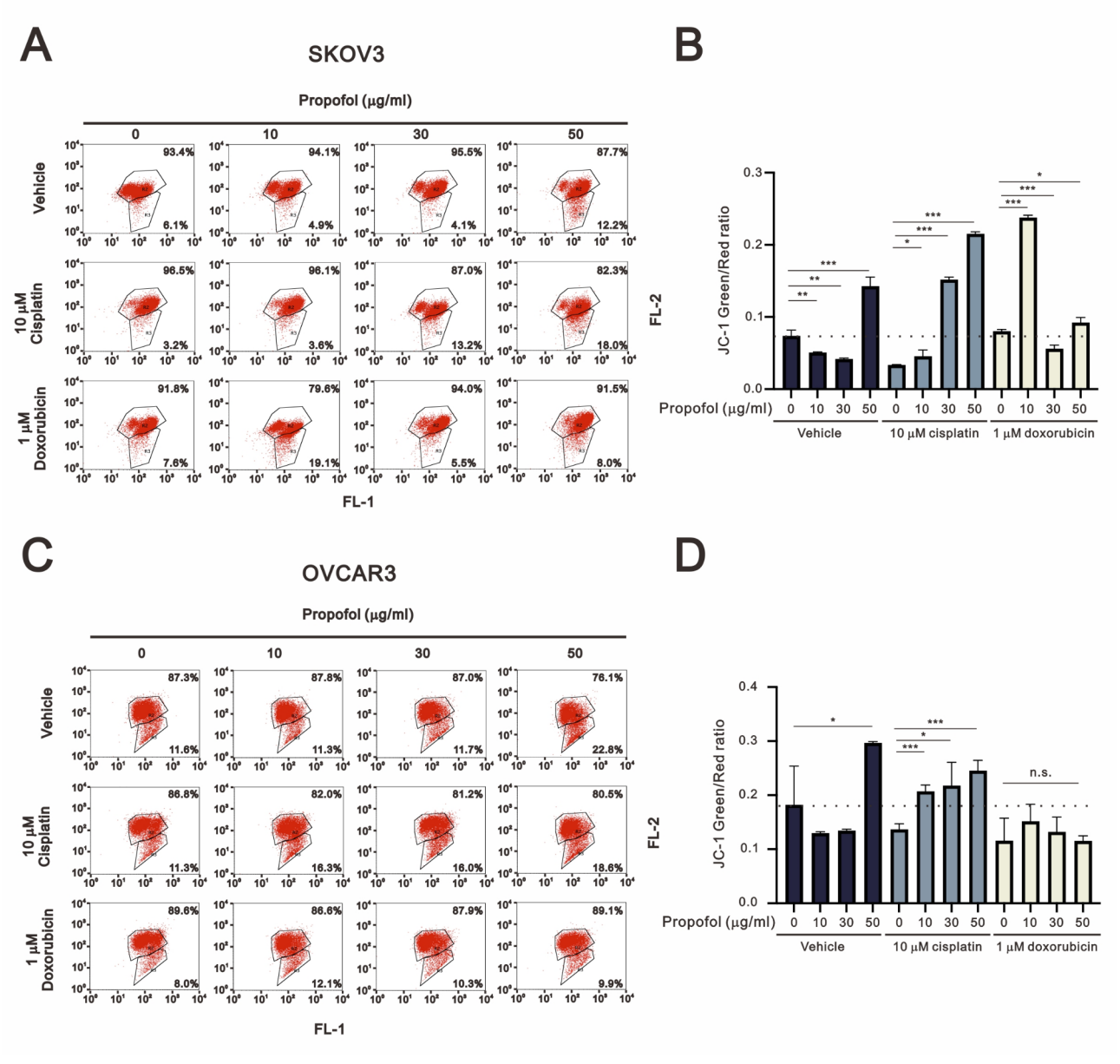

Fig. 4 The mitochondrial membrane potential of human ovarian cancer cells was assessed upon exposure to propofol combined with cisplatin or doxorubicin. SKOV3 and OVCAR3 cells were treated with different concentrations of propofol (0, 10, 30, and 50 μg/ml) in combination with either 10 μM cisplatin or 1 μM doxorubicin for 24 h. Then, the cells were analyzed using flow cytometry with JC-1 staining. The bars represent the mean ± SD of three independent experiments. Statistical significance is indicated by * for $p < 0.05$, ** for $p < 0.01$, and *** for $p < 0.001$, determined using Student's *t*-tests

ovarian cancer cells (Fig. 7). The results showed that 50 μg/ml propofol significantly inhibited the migration ability of SKOV3 and OVCAR3 cells (Fig. 7B and D).

SKOV3 cells, a p53-null cell line, exhibited a phenotype typical of mesenchymal cells, while OVCAR3 cells showed strong expression of E-Cadherin, not vimentin, and displayed epithelial morphology [42]. We confirmed the absence of endogenous p53 and vimentin protein in SKOV3 cells and OVCAR3 cells, respectively. We further checked the expression of related proteins associated with EMT, such as snail, vimentin, α-SMA (a target of TGF-β pathway), and E-cadherin, as well as markers of cellular stresse including γ-H2A.x, p53, cyclin D1, and p-ERK/ERK, using Western blotting analysis in SKOV3 and OVCAR3 cells (Fig. 8). Propofol increased the protein expression of γ-H2A.x, cyclin D1, and p-ERK in SKOV3 cells, and α-SMA and p-ERK in OVCAR3 cells. In SKOV3 cells, propofol decreased the protein expression of snail, E-cadherin, ERK, and α-tubulin, whereas propofol decreased γ-H2A.x and cyclin D1 in OVCAR3 cells. Cisplatin decreased the protein expression of snail, α-SMA, E-cadherin, γ-H2A.x, and ERK, and increased

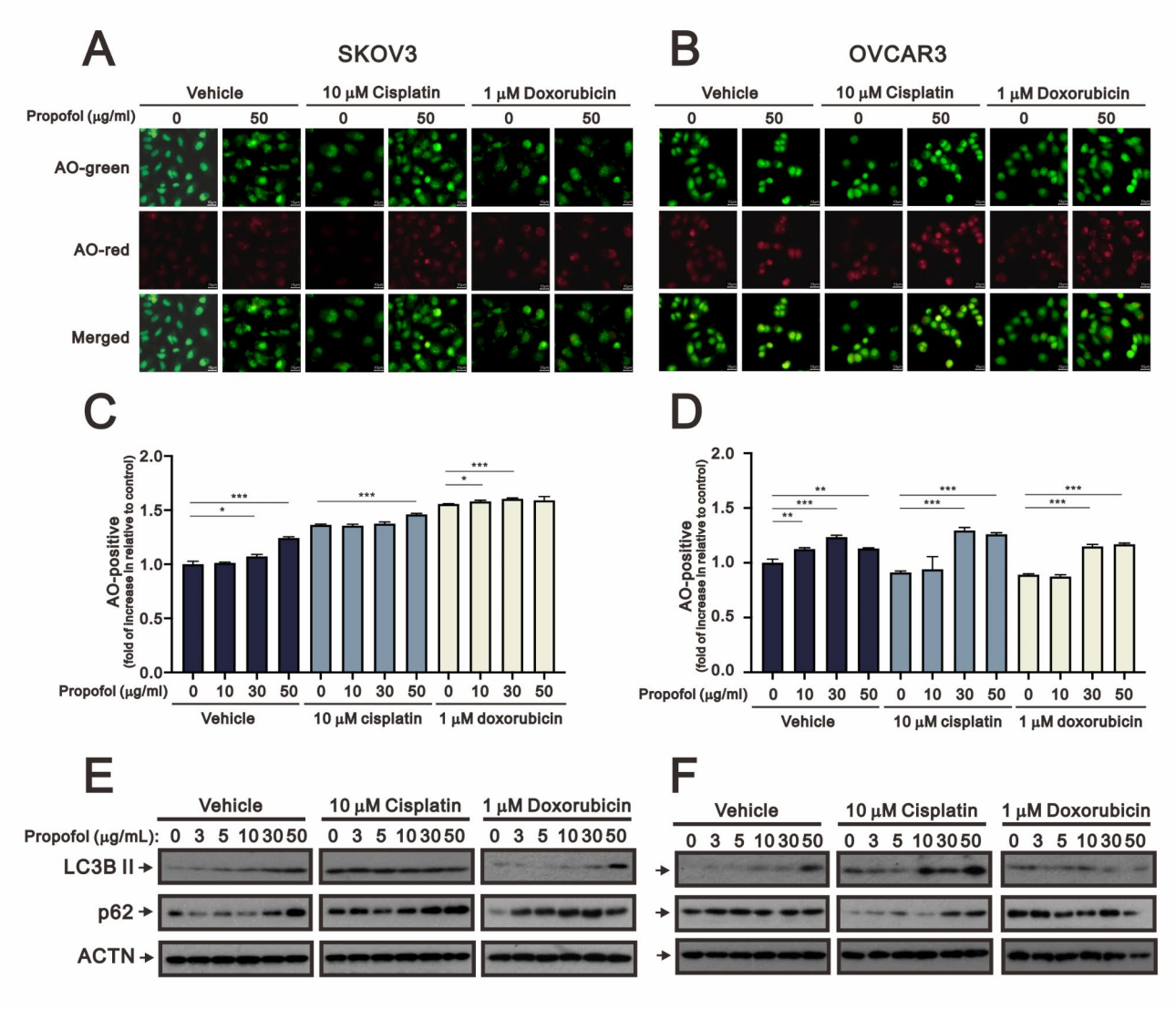

Fig. 5 The effects of propofol in combination with cisplatin and doxorubicin on autophagy in human ovarian cells. (**A-B**) Fluorescence microscopy images of SKOV3 and OVCAR3 cells treated with propofol at concentrations of 0 and 50 μg/ml, and stained with AO, are shown (scale bar: 10 μm). (**C-D**) SKOV3 and OVCAR3 cells treated with propofol at concentrations of 0, 10, 30, and 50 μg/ml combined with either 10 μM cisplatin or 1 μM doxorubicin for 24 h were analyzed using flow cytometry with AO staining. The bars represent the mean ± SD of three independent experiments. Statistical significance is indicated by * for $p < 0.05$, ** for $p < 0.01$, and *** for $p < 0.001$, determined using Student's *t*-tests. Cell lysates of (**E**) SKOV3 and (**F**) OVCAR3 were subjected to Western blot analysis using antibodies against the indicated proteins. ACTN was the protein loading control

cyclin D1 and p-ERK in SKOV3 cells. In OVCAR3 cells, cisplatin decreased the protein expression of cyclin D1 and increased snail, α-SMA, γ-H2A.x, and p-ERK. Doxorubicin decreased the protein expression of vimentin, α-SMA, and E-cadherin, and increased γ-H2A.x, cyclin D1, and p-ERK in SKOV3 cells. In OVCAR3 cells, doxorubicin decreased the protein expression of cyclin D1 and increased snail, α-SMA, γ-H2A.x, and p-ERK. In SKOV3 cells, propofol combined with cisplatin, resulting in similar trends as propofol alone, such as α-SMA, E-cadherin, γ-H2A.x, ERK, and p-ERK; propofol combined with doxorubicin in the only decreasing trend of E-cadherin had with propofol alone, and with predominant effects on snail, vimentin, α-SMA, p-ERK, and ERK that doxorubicin had. The levels of cisplatin- and doxorubicin-induced γ-H2A.x proteins were reduced with increasing amounts of propofol in OVCAR3 cells, while doxorubicin-induced γ-H2A.x proteins were reduced with increasing amounts of propofol in SKOV3 cells.

Discussion

It is a growing clinical challenge to prevent the development of resistance to cisplatin or doxorubicin by ovarian cancer cells. Hence, it is urgent to find methods of increasing the efficiency and effectiveness of the cytotoxic effects of cisplatin or doxorubicin to inhibit the

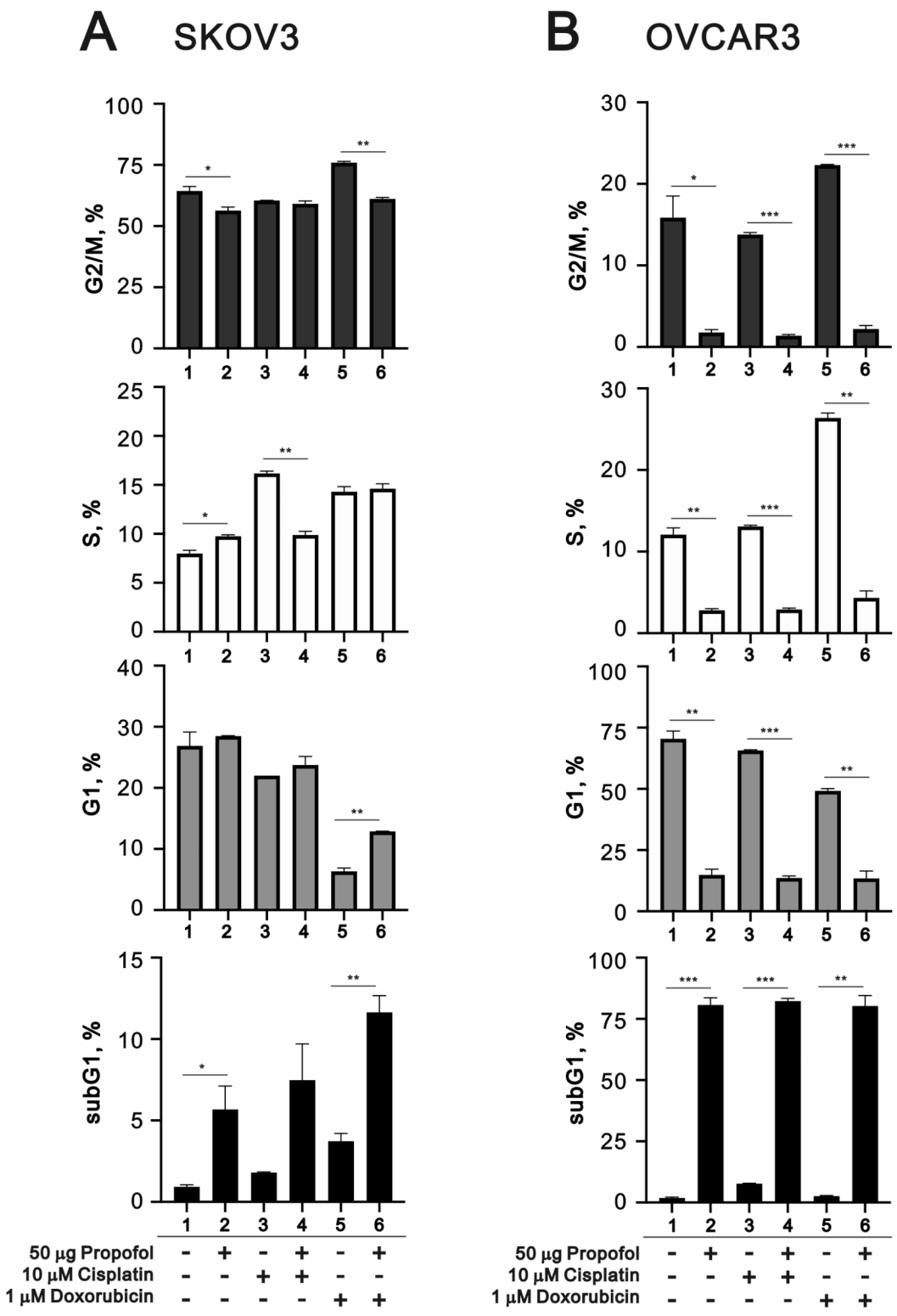

Fig. 6 The impact of propofol in combination with cisplatin and doxorubicin on the cell cycle profile in human ovarian cells. (**A-B**) After treating SKOV3 and OVCAR3 cells with concentrations of propofol (0 and 50 µg/ml) in combination with either 10 µM cisplatin or 1 µM doxorubicin for 24 h, PI staining was performed, and the cells were analyzed using flow cytometry. The bars represent the mean ± SD of three independent experiments. Statistical significance is indicated by * for $p < 0.05$, ** for $p < 0.01$, and *** for $p < 0.001$, determined using Student's *t*-tests

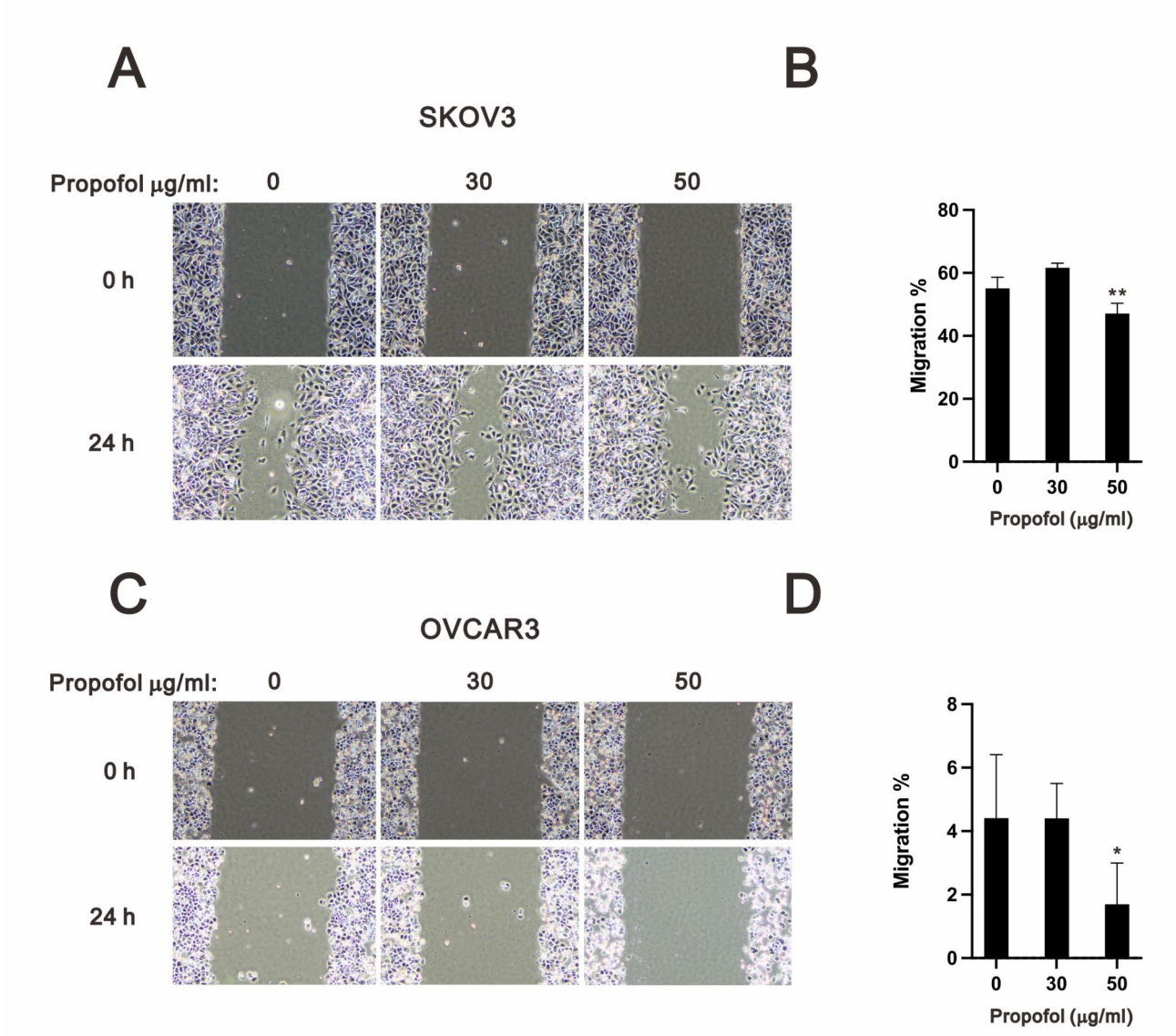

Fig. 7 Analysis of the effect of propofol on the cell migration of human ovarian cancer cells. SKOV3 and OVCAR3 cells were treated with propofol (0, 30, and 50 µg/ml) for 24 h. Images were captured using the ECLIPSE Ts2 inverted microscope at 0 and 24 h. Quantification of the migration area of untreated and propofol-treated cells within 24 h using Image J. Bars depict the mean ± SD of three independent experiments. * $p < 0.05$ and ** $p < 0.01$ (Student's *t*-tests)

mechanisms of resistance developed by cancer cells and restore the sensitivity of these cells. Drug repurposing has now become a powerful and efficient alternative strategy for the development of these candidates. The findings of this study demonstrated that propofol had potential cytotoxic properties and inhibited the colony formation, cell viability, and migratory ability of human ovarian cancer cells. Furthermore, the synergistic effects of propofol in combination therapy with either cisplatin or doxorubicin in human ovarian cancer cell lines were observed. Regarding the potential correlation between propofol and human ovarian cancer cells, Hu and colleagues demonstrated that propofol in vitro negatively modulated cellular signaling pathways and inhibited the metabolic efficiency of human ovarian cancer cells, which eventually decreased cancer malignancy [43]. Propofol could also inhibit proliferation, migration, and invasion, as well as induce apoptosis in human ovarian cancer cell lines by regulating key RNA expression, and subsequently affecting related signaling pathways [44–48]. Moreover, propofol treatment in vitro was shown to reduce cisplatin resistance and promote paclitaxel sensitivity in human ovarian cancer cells [49, 50].

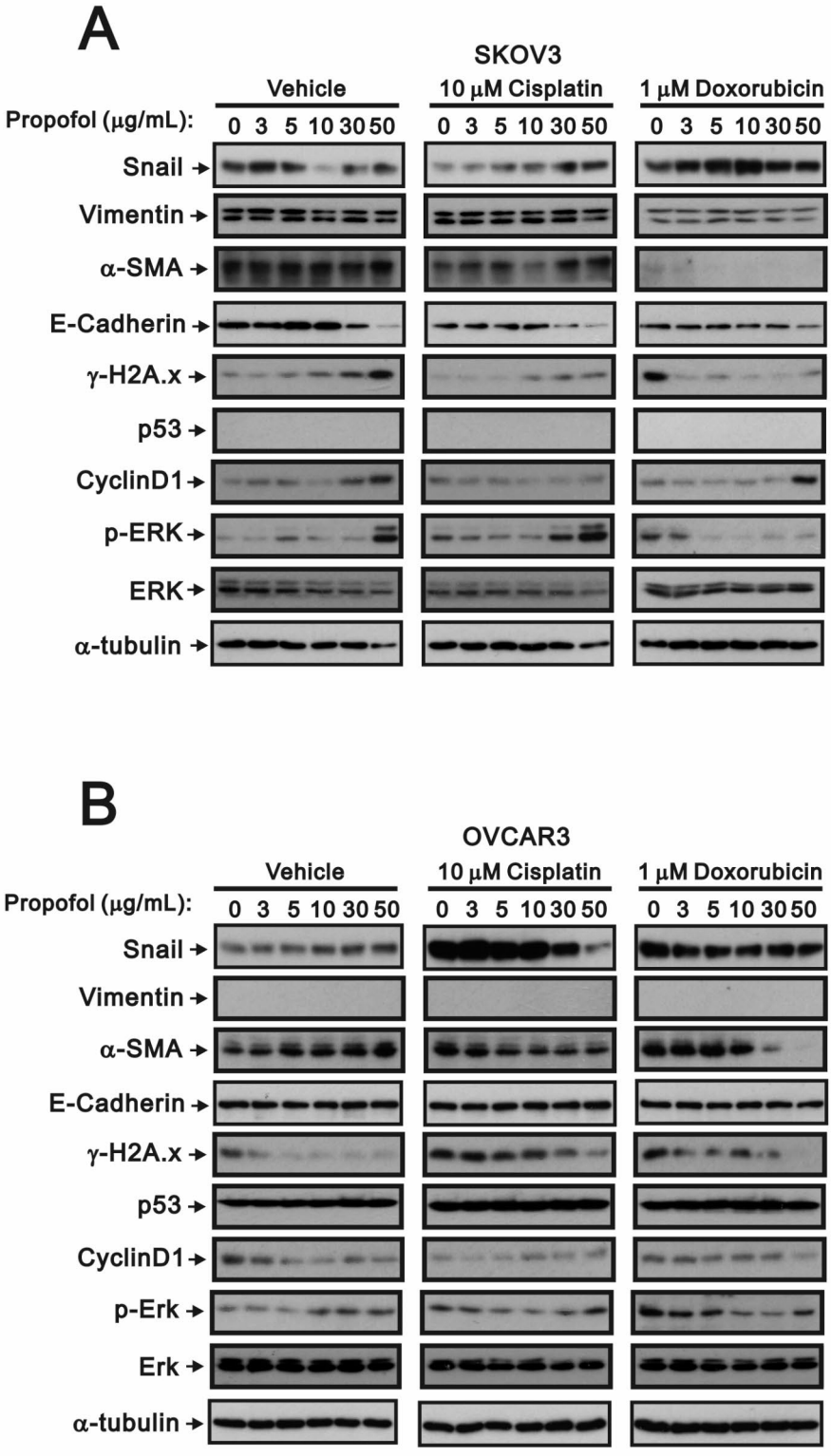

Fig. 8 The impact of propofol in combination with cisplatin or doxorubicin on the protein expression in human ovarian cancer cells. (**A**) SKOV3 and (**B**) OVCAR3 cells treated with propofol at concentrations of 0 and 50 μg/ml, combined with either 10 μM cisplatin or 1 μM doxorubicin, for a duration of 24 h. Cell lysates were subjected to Western blot analysis using antibodies against the indicated proteins. α-tubulin was used as the loading control

In this study, the cell viability of human ovarian cancer cells was found to be dose-dependently decreased with an increased concentration of propofol, in agreement with the findings of previous studies [44–50]. Additionally, we demonstrated a novel therapeutic strategy by combining propofol with either cisplatin or doxorubicin for investigating the treatment efficiency of ovarian cancer. Our results indicated the synergistic cytotoxicity of propofol administration with cisplatin or doxorubicin in SKOV3 and OVCAR3 cells. Sun and colleagues demonstrated that propofol could enhance chemo-sensitivity in both cisplatin-sensitive and -resistant human ovarian cancer cells through regulating the microRNA 374a/forkhead box O1 signaling axis [49]. Similarly, propofol was reported to increase paclitaxel-induced cytotoxicity in both resistant and sensitive human ovarian cancer cells through the suppression of the transcription factor slug [50]. These findings could be translated into an alternative to diminish the adverse effect profile and lower the risk of chemo-resistance in ovarian cancer. However, further in vivo and clinical studies are necessary to elucidate the optimal dosages of propofol, followed by chemotherapeutic agents, for combination therapy in ovarian cancer, especially for advanced ovarian cancer.

Colony formation is an in vitro cell survival assay based on the ability of every cell in the population to undergo unlimited division, which is the method of choice to determine cell survival and growth after treatment with ionizing radiation, or to determine the effectiveness of cytotoxic agents [51]. To identify the impact of anchorage-independent growth by propofol, we conducted a colony formation analysis, showing that colony formation of SKOV3 and OVCAR3 cells was significantly inhibited following treatment with propofol (at concentrations of more than 40 and more than 30 μg/ml, respectively) in a dose-dependent manner. A previous in vitro study has also demonstrated that propofol dose-dependently inhibited the colony formation ability of human ovarian cancer cells; nevertheless, propofol-inhibited colony formation ability was partly recovered by the overexpression of circular RNA mucin 16, which mediated the miR-1182/S100B signaling pathway [48]. In addition, similar results of decreased colony formation were shown in other cancer cell lines treated with propofol [52–55]. Taken together, propofol seems to exert a potent inhibitory effect on the cellular proliferation of human ovarian cancer cells.

Compared with the ED50 values of 54.6 μg/ml for propofol, 31.6 μM for cisplatin, and 0.8 μM for doxorubicin in SKOV3 cells, and 19 μg/ml, 9.4 μM, and 3.2 μM in OVCAR3 cells (Fig. 1), we applied 10, 30, and 50 μg/ml propofol, 10 μM cisplatin, and 1 μM doxorubicin to examine their effects on apoptotic populations. The induction of early and late apoptosis by propofol was observed at a minimum concentration of 10 μg/ml in SKOV3 cells and 50 μg/ml in OVCAR3 cells (Fig. 3), whereas 10 μg/ml propofol suppressed colony formation in both cell lines (Fig. 2). The sensitivity of ovarian cancer cells to cisplatin or doxorubicin for the induction of apoptosis may depend on the status of p53. In Fig. 3, cisplatin and doxorubicin induced early and late apoptosis in p53-null SKOV3 cells, while cisplatin had no effect and doxorubicin suppressed early and late apoptosis in OVCAR3 cells. Cisplatin had no effect on propofol-induced early and late apoptosis in SKOV3 cells but suppressed propofol-induced early and late apoptosis in OVCAR3 cells. Doxorubicin potentiated propofol-induced early apoptosis in both cells and potentiated late apoptosis in SKOV3 cells, while suppressing late apoptosis in OVCAR3 cells. When comparing the population of the subG1 phase (Fig. 6), propofol, cisplatin, and doxorubicin all increased the populations of the subG1 phase, and cisplatin and doxorubicin enhanced the effect of propofol on the subG1 phase in SKOV3 cells. Only propofol and cisplatin increased the populations of the subG1 phase, while doxorubicin had no effect on the propofol-induced subG1 populations in OVCAR3 cells.

Autophagy involves several sequential steps: initiation, membrane nucleation, elongation for autophagosome formation (maturation), and fusion with lysosomes to form autophagolysosomes for degradation and recycling. Our OA-red staining results, which indicate autophagolysosomes, were consistent with the LC3BII amount (indicating elongation for autophagosome formation). However, while p62 protein is involved in the initiation of autophagy, it also serves as a cargo for degradation. Our current findings suggest that p62 protein may be involved only in the initiation of autophagy, and its primary degradation may not occur through autophagy. In SKOV3 cells, propofol, cisplatin, and doxorubicin are involved in the process of elongation for autophagosome formation and autophagolysosome formation. Cisplatin and doxorubicin potentiated the effects of propofol on these two processes of autophagy. In OVCAR3 cells, propofol, cisplatin, and doxorubicin are involved in the process of elongation for autophagosome formation, and cisplatin potentiated the effects of propofol on autophagolysosome formation.

Inherited genetic mutations (such as p53 gene), altered oxidative stress, mitochondrial dysregulation, and decreased apoptosis lead to the development of ovarian cancer. The vast majority of cancer-associated p53 mutants are full-length proteins, typically with only a single amino acid mutation within its DNA binding domain, including residues 175, 248, and 273. The sensitivity of chemotherapy is also reported to be p53-dependent [29, 30]. In addition to p53 gain-of-function mutants, high vimentin expression indicates prolonged survival in

patients with ovarian cancers because of the improved sensitivity to platinum-based agents [56, 57]. Two human ovarian cancer cell lines with various p53 characteristics, p53-null (SKOV-3) and mutant p53 (R248Q) (OVCAR-3), were used in this study. In our Western blotting data, vimentin proteins were difficult to detect, and E-cadherin proteins were easy to detect in OVCAR-3 cells [57, 58]. The detectable presence of both vimentin and E-cadherin proteins in SKOV3 suggests that the expressions of these proteins are dependent on the specific ovarian cancer types. The process of EMT is closely related to autophagy by regulating metabolic stress and other micro-environmental changes in various cancers [59]. Autophagy is a degradation process to reduce stress and maintain proper cell function. p53 possesses dual functions in autophagy-mediated apoptosis, or survive in a transcription-dependent and -independent manner, which were observed for autophagy-dependent drug resistance of chemotherapy-exposed tumor cells [60]. However, autophagy has a controversial function in cancer in suppressing the viability and proliferation of cancer cells.

Based on the combination index, propofol and cisplatin were more sensitive in OVCAR3 cells than in SKOV3 cells, while doxorubicin was more sensitive in SKOV3 cells than in OVCAR3 cells. Consequently, doxorubicin exhibited insensitivity in the analysis of apoptosis, autophagy, and mitochondrial membrane potential in OVCAR3 cells. Additionally, doxorubicin played a suppressive role in the propofol-induced effects on these functions. Our data also indicated that the effects of 50 μg/ml propofol on colony formation and migration might not be mediated through cytotoxicity, as it induced apoptosis, disrupted mitochondrial membrane potential and autophagy, and altered some protein expressions in both cell lines. In our data for SKOV3 and OVCAR3 cells, propofol had different effects on the combination index, mitochondrial membrane potential, autophagy, apoptosis, cell cycle profile, and EMT. Thus, these aspects of crosstalk among p53 status, EMT, autophagy, mitochondrial membrane potential, and chemo-resistance of cisplatin and doxorubicin are particularly intriguing, and demand further investigation.

Conclusions

This study aimed to uncover the antitumor effects of propofol alone and combined with cisplatin or doxorubicin in SKOV3 and OVCAR3 human ovarian cancer cells. First, propofol demonstrated synergistic interactions with cisplatin and doxorubicin in SKOV3 cells, while in OVCAR3 cells, synergy was observed only with doxorubicin. Subsequently, our findings revealed that propofol suppressed colony formation, disrupted mitochondrial membrane potential, and induced apoptosis and autophagy in SKOV3 and OVCAR3 cells. Furthermore, the effects of propofol combined with cisplatin or doxorubicin on mitochondrial membrane potential, apoptosis, autophagy, and EMT differed between SKOV3 and OVCAR3 cells, depending on the p53 status. In summary, repurposing propofol shows potential for overcoming resistance to cisplatin or doxorubicin, potentially reducing the required chemotherapy dosages and associated side effects, thus improving treatment outcomes.

Acknowledgements
No applicable.

Author contributions
JLC, ZFW, and HCL contributed to the conceptualization, supervision, and editing of the final manuscript. SHS, WCT, ZSW, and SMH contributed to the investigation, methodology, validation, original draft preparation, and revision of the manuscript. JLC, ZFW, and SMH contributed to the funding acquisition. All authors have read and approved the final version of this manuscript.

Funding
This work was supported by grants from the National Science and Technology Council [NSTC 112-2635-B016-002 to J-L Chen], the Teh-Tzer Study Group for Human Medical Research Foundation [A1111035 to S-M Huang], and the Kaohsiung Medical University Hospital (KMUHIRB-F(II)-20220157 to Z-F Wu), Taiwan, Republic of China.

Data availability
The data generated in this study are available within the paper. Derived data supporting the findings of this study are available upon reasonable requests from the corresponding author.

Declarations

Conflict of interest
The authors declare no conflict of interest.

Competing interests
The authors declare no competing interests.

Author details
[1]Department of Surgery, Taipei City Hospital Renai Branch, Taipei City 106, Taiwan, Republic of China
[2]Department of Anesthesiology, Tri-Service General Hospital, National Defense Medical Center, Taipei City 114, Taiwan, Republic of China
[3]Institute of Life Sciences, National Defense Medical Center, Taipei City 114, Taiwan, Republic of China
[4]Department of Biochemistry, National Defense Medical Center, Taipei City 114, Taiwan, Republic of China
[5]Department of Anesthesiology, Kaohsiung Medical University Hospital, Kaohsiung Medical University, Kaohsiung City 807, Taiwan, Republic of China
[6]Department of Anesthesiology, Faculty of Medicine, College of Medicine, Kaohsiung Medical University, Kaohsiung City 807, Taiwan, Republic of China
[7]Center for Regional Anesthesia and Pain Medicine, Wan Fang Hospital, Taipei Medical University, Taipei City 116, Taiwan, Taiwan, Republic of China

Received: 17 January 2024 / Accepted: 31 August 2024
Published online: 14 September 2024

References

1. Lheureux S, Braunstein M, Oza AM. Epithelial ovarian cancer: evolution of management in the era of precision medicine. CA Cancer J Clin. 2019;69(4):280–304.

2. Gaona-Luviano P, Medina-Gaona LA, Magaña-Pérez K. Epidemiology of ovarian cancer. Chin Clin Oncol. 2020;9(4):47.
3. Torre LA, Trabert B, DeSantis CE, Miller KD, Samimi G, Runowicz CD, Gaudet MM, Jemal A, Siegel RL. Ovarian cancer statistics, 2018. CA Cancer J Clin. 2018;68(4):284–96.
4. Lheureux S, Gourley C, Vergote I, Oza AM. Epithelial ovarian cancer. Lancet. 2019;393(10177):1240–53.
5. Kim R. Effects of surgery and anesthetic choice on immunosuppression and cancer recurrence. J Translational Med. 2018;16(1):8.
6. Chen Z, Zhang P, Xu Y, Yan J, Liu Z, Lau WB, Lau B, Li Y, Zhao X, Wei Y. Surgical stress and cancer progression: the twisted tango. Mol Cancer. 2019;18(1):1–11.
7. Liu X, Wang Q. Application of anesthetics in Cancer patients: reviewing current existing Link with Tumor recurrence. Front Oncol. 2022;12:759057.
8. Xu YJ, Li SY, Cheng Q, Chen WK, Wang SL, Ren Y, Miao CH. Effects of anaesthesia on proliferation, invasion and apoptosis of LoVo colon cancer cells in vitro. Anaesthesia. 2016;71(2):147–54.
9. Soltanizadeh S, Degett TH, Gogenur I. Outcomes of cancer surgery after inhalational and intravenous anesthesia: a systematic review. J Clin Anesth. 2017;42:19–25.
10. Yap A, Lopez-Olivo MA, Dubowitz J, Hiller J, Riedel B. Global onco-anesthesia research collaboration G: anesthetic technique and cancer outcomes: a meta-analysis of total intravenous versus volatile anesthesia. Can J Anaesth. 2019;66(5):546–61.
11. Ramirez MF, Cata JP. Anesthesia techniques and long-term oncological outcomes. Front Oncol. 2021;11:788918.
12. Chang CY, Wu MY, Chien YJ, Su IM, Wang SC, Kao MC. Anesthesia and long-term oncological outcomes: a systematic review and Meta-analysis. Anesth Analg. 2021;132(3):623–34.
13. Zhou X, Shao Y, Li S, Zhang S, Ding C, Zhuang L, Sun J. An intravenous anesthetic drug-propofol, influences the biological characteristics of malignant tumors and reshapes the tumor microenvironment: a narrative literature review. Front Pharmacol. 2022;13:1057571.
14. Xu Y, Pan S, Jiang W, Xue F, Zhu X. Effects of propofol on the development of cancer in humans. Cell Prolif. 2020;53(8):e12867.
15. Jiang S, Liu Y, Huang L, Zhang F, Kang R. Effects of propofol on cancer development and chemotherapy: potential mechanisms. Eur J Pharmacol. 2018;831:46–51.
16. Tseng W-C, Lee M-S, Lin Y-C, Lai H-C, Yu M-H, Wu K-L, Wu Z-F. Propofol-based total intravenous anesthesia is Associated with Better Survival than Desflurane Anesthesia in epithelial ovarian Cancer surgery: a retrospective cohort study. Front Pharmacol. 2021;12:685265.
17. Zon A, Bednarek I. Cisplatin in ovarian cancer treatment-known limitations in therapy force new solutions. Int J Mol Sci. 2023;24(8):7585.
18. Basu A, Krishnamurthy S. Cellular responses to Cisplatin-induced DNA damage. *J Nucleic Acids* 2010, 2010:201367.
19. Dasari S, Tchounwou PB. Cisplatin in cancer therapy: molecular mechanisms of action. Eur J Pharmacol. 2014;740:364–78.
20. Guarneri V, Piacentini F, Barbieri E, Conte PF. Achievements and unmet needs in the management of advanced ovarian cancer. Gynecol Oncol. 2010;117(2):152–8.
21. Galluzzi L, Senovilla L, Vitale I, Michels J, Martins I, Kepp O, Castedo M, Kroemer G. Molecular mechanisms of cisplatin resistance. Oncogene. 2012;31(15):1869–83.
22. Lawrie TA, Bryant A, Cameron A, Gray E, Morrison J. Pegylated liposomal doxorubicin for relapsed epithelial ovarian cancer. Cochrane Database Syst Rev. 2013;2013(7):CD006910.
23. Nitiss JL. Targeting DNA topoisomerase II in cancer chemotherapy. Nat Rev Cancer. 2009;9(5):338–50.
24. Bayat Mokhtari R, Homayouni TS, Baluch N, Morgatskaya E, Kumar S, Das B, Yeger H. Combination therapy in combating cancer. Oncotarget. 2017;8(23):38022–43.
25. Pritchard JR, Bruno PM, Gilbert LA, Capron KL, Lauffenburger DA, Hemann MT. Defining principles of combination drug mechanisms of action. Proc Natl Acad Sci U S A. 2013;110(2):E170–179.
26. Mammoto T, Mukai M, Mammoto A, Yamanaka Y, Hayashi Y, Mashimo T, Kishi Y, Nakamura H. Intravenous anesthetic, propofol inhibits invasion of cancer cells. Cancer Lett. 2002;184(2):165–70.
27. Kushida A, Inada T, Shingu K. Enhancement of antitumor immunity after propofol treatment in mice. Immunopharmacol Immunotoxicol. 2007;29(3–4):477–86.
28. Pushpakom S, Iorio F, Eyers PA, Escott KJ, Hopper S, Wells A, Doig A, Guilliams T, Latimer J, McNamee C, et al. Drug repurposing: progress, challenges and recommendations. Nat Rev Drug Discov. 2019;18(1):41–58.
29. El-Deiry WS. The role of p53 in chemosensitivity and radiosensitivity. Oncogene. 2003;22(47):7486–95.
30. Hientz K, Mohr A, Bhakta-Guha D, Efferth T. The role of p53 in cancer drug resistance and targeted chemotherapy. Oncotarget. 2017;8(5):8921–46.
31. Cocetta V, Ragazzi E, Montopoli M. Mitochondrial involvement in Cisplatin Resistance. Int J Mol Sci. 2019;20(14):3384.
32. Zong WX, Rabinowitz JD, White E. Mitochondria and Cancer. Mol Cell. 2016;61(5):667–76.
33. Guerra F, Arbini AA, Moro L. Mitochondria and cancer chemoresistance. Biochim Biophys Acta Bioenerg. 2017;1858(8):686–99.
34. Srinivasan S, Guha M, Kashina A, Avadhani NG. Mitochondrial dysfunction and mitochondrial dynamics-the cancer connection. Biochim Biophys Acta Bioenerg. 2017;1858(8):602–14.
35. Kingnate C, Charoenkwan K, Kumfu S, Chattipakorn N, Chattipakorn SC. Possible Roles of Mitochondrial Dynamics and the effects of pharmacological interventions in Chemoresistant Ovarian Cancer. EBioMedicine. 2018;34:256–66.
36. Yu L, Chen Y, Tooze SA. Autophagy pathway: Cellular and molecular mechanisms. Autophagy. 2018;14(2):207–15.
37. Devenish RJ, Klionsky DJ. Autophagy: mechanism and physiological relevance 'brewed' from yeast studies. Front Biosci (Schol Ed). 2012;4(4):1354–63.
38. Kriel J, Loos B. The good, the bad and the autophagosome: exploring unanswered questions of autophagy-dependent cell death. Cell Death Differ. 2019;26(4):640–52.
39. Denton D, Kumar S. Autophagy-dependent cell death. Cell Death Differ. 2019;26(4):605–16.
40. Tiwari N, Gheldof A, Tatari M, Christofori G. EMT as the ultimate survival mechanism of cancer cells. Semin Cancer Biol. 2012;22(3):194–207.
41. Yang J, Antin P, Berx G, Blanpain C, Brabletz T, Bronner M, Campbell K, Cano A, Casanova J, Christofori G, et al. Guidelines and definitions for research on epithelial-mesenchymal transition. Nat Rev Mol Cell Biol. 2020;21(6):341–52.
42. De Haven Brandon A, Box G, Hallsworth A, Court W, Matthews N, Herodek B, Arteagabeitia AB, Valenti M, Kirkin V. Identification of ovarian high-grade serous carcinoma cell lines that show estrogen-sensitive growth as xenografts in immunocompromised mice. Sci Rep. 2020;10(1):10799.
43. Hu C, Wang B, Liu Z, Chen Q, Ishikawa M, Lin H, Lian Q, Li J, Li JV, Ma D. Sevoflurane but not propofol enhances ovarian cancer cell biology through regulating cellular metabolic and signaling mechanisms. Cell Biol Toxicol. 2023;39(4):1395–411.
44. Huang X, Teng Y, Yang H, Ma J. Propofol inhibits invasion and growth of ovarian cancer cells via regulating miR-9/NF-κB signal. Braz J Med Biol Res. 2016;49(12):e5717.
45. Zeng J, Li YK, Quan FF, Zeng X, Chen CY, Zeng T, Zou J, Tong WJ. Propofol–induced miR–125a–5p inhibits the proliferation and metastasis of ovarian cancer by suppressing LIN28B. Mol Med Rep. 2020;22(2):1507–17.
46. Shen X, Wang D, Chen X, Peng J. Propofol inhibits proliferation, migration, invasion and promotes apoptosis by regulating HOST2/JAK2/STAT3 signaling pathway in ovarian cancer cells. Cytotechnology. 2021;73(2):243–52.
47. Lu H, Zheng G, Gao X, Chen C, Zhou M, Zhang L. Propofol suppresses cell viability, cell cycle progression and motility and induces cell apoptosis of ovarian cancer cells through suppressing MEK/ERK signaling via targeting circVPS13C/miR-145 axis. J Ovarian Res. 2021;14(1):30.
48. Yang H, Guo Y, Zhang Y, Wang D, Zhang G, Hou J, Yang J. Circ_MUC16 attenuates the effects of Propofol to promote the aggressive behaviors of ovarian cancer by mediating the miR-1182/S100B signaling pathway. BMC Anesthesiol. 2021;21(1):297.
49. Sun Y, Peng YB, Ye LL, Ma LX, Zou MY, Cheng ZG. Propofol inhibits proliferation and cisplatin resistance in ovarian cancer cells through regulating the microRNA–374a/forkhead box O1 signaling axis. Mol Med Rep. 2020;21(3):1471–80.
50. Wang P, Chen J, Mu LH, Du QH, Niu XH, Zhang MY. Propofol inhibits invasion and enhances paclitaxel- induced apoptosis in ovarian cancer cells through the suppression of the transcription factor slug. Eur Rev Med Pharmacol Sci. 2013;17(13):1722–9.
51. Franken NA, Rodermond HM, Stap J, Haveman J, van Bree C. Clonogenic assay of cells in vitro. Nat Protoc. 2006;1(5):2315–9.
52. Xiao G, Yu L, Tan W, Yang H, Li W, Xia R, Li Y. Propofol inhibits glioma progression by regulating circMAPK4/miR-622/HOXA9 axis. Metab Brain Dis. 2023;38(1):233–44.

53. Zhang X, Liu D, Wang P, Liu N. Propofol mediates non-small cell lung cancer growth in part by regulating circ_0003028-related mechanisms. Thorac Cancer. 2023;14(17):1606–17.
54. Sun N, Zhang W, Liu J, Yang X, Chu Q. Propofol inhibits the progression of Cervical Cancer by regulating HOTAIR/miR-129-5p/RPL14 Axis. Onco Targets Ther. 2021;14:551–64.
55. Liu YP, Qiu ZZ, Li XH, Li EY. Propofol induces ferroptosis and inhibits malignant phenotypes of gastric cancer cells by regulating miR-125b-5p/STAT3 axis. World J Gastrointest Oncol. 2021;13(12):2114–28.
56. Szubert S, Koper K, Dutsch-Wicherek MM, Jozwicki W. High tumor cell vimentin expression indicates prolonged survival in patients with ovarian malignant tumors. Ginekol Pol. 2019;90(1):11–9.
57. Lai ZY, Tsai KY, Chang SJ, Chuang YJ. Gain-of-function mutant TP53 R248Q overexpressed in epithelial ovarian carcinoma alters AKT-dependent regulation of intercellular trafficking in responses to EGFR/MDM2 inhibitor. Int J Mol Sci. 2021;22(16):8784.
58. Lee JG, Ahn JH, Jin Kim T, Ho Lee J, Choi JH. Mutant p53 promotes ovarian cancer cell adhesion to mesothelial cells via integrin beta4 and Akt signals. Sci Rep. 2015;5:12642.
59. Chen HT, Liu H, Mao MJ, Tan Y, Mo XQ, Meng XJ, Cao MT, Zhong CY, Liu Y, Shan H, et al. Crosstalk between autophagy and epithelial-mesenchymal transition and its application in cancer therapy. Mol Cancer. 2019;18(1):101.
60. Jin S. p53, autophagy and tumor suppression. Autophagy. 2005;1(3):171–3.

Publisher's note

Springer Nature remains neutral with regard to jurisdictional claims in published maps and institutional affiliations.